Latin American Journal of Solids and Structures
www.lajss.org

A study on the nonlinear stability of orthotropic single-layered graphene sheet based on nonlocal elasticity theory

Abstract

Recently, graphene sheets have shown significant potential for environmental engineering applications such as wastewater treatment. In the present work, the posbuckling response of orthotropic single-layered graphene sheet (SLGS) is investigated in a closed-form analytical manner using the nonlocal theory of Eringen. Two opposite edges of the plate are subjected to normal stresses. The nonlocality and geometric nonlinearity are taken into consideration, which arises from the nanosized effects and mid-plane stretching, respectively. Nonlinear governing differential equations (nonlocal compatibility and equilibrium equations) are derived and presented for the aforementioned study. Galerkin method is used to solve the governing equations for simply supported boundary conditions. It is shown that the nonlocal effect plays a significant role in the nonlinear stability behavior of orthotropic nanoplates. Unlike first and second postbuckling modes, nonlocal effects decrease with the increase of lateral deflection at higher postbuckling modes. It is also observed that the nonlocality and nonlinearity is more pronounced for higher postbuckling modes.

Keywords

Postbuckling, Orthotropic nanoplates, Small scale effect, Nonlocal plate theory.

S.R. Asemi [a]
M. Mohammadi [b, *]
A. Farajpour [c]

[a] Department of Environment, Damavand Branch, Islamic Azad University, Damavand, Iran

[b] Department of engineering, Ahvaz branch, Islamic Azad University, Ahvaz, Iran

[c] Young Researchers and Elites Club, North Tehran Branch, Islamic Azad University, Tehran, Iran

*Author email: m.mohamadi@me.iut.ac.ir

1 INTRODUCTION

Since the discovery of carbon nanotubes (CNTs) by Iijima (1991), many scientific researches have been carried out in the field of mechanical, electrical, physical and chemical properties of nanostructures. In-depth studies on the nanomaterials have shown that their mechanical characteristics are different from other well-known materials (Miller and Shenoy 2000). The desirable properties of nanostructures make them favorable for nanoengineering applications in many fields such as nanodevices, nanosensors, nanooscillators, nanoactuators, nanobearings, hydrogen storage, atomic-

force microscope, electrical batteries and nanocomposites (Craighead 2000; Li et al. 2007; Murmu and Adhikari 2010). In addition, nanostructures such as armchair carbon nanotubes and nanoplates have shown significant potential applications in the field of environmental technologies (Saremi et al. 2008).

Continuum based analyses of nanostructures have been widely used for the formulation of various dynamic and stability problems at small scales. The two main reasons for this are that experimental investigations in nanoscale are difficult and molecular dynamic (MD) simulations are highly computationally expensive for nanostructures with large numbers of atoms or molecules inside them. Over the past decade, some researchers have applied classical continuum mechanics such as Euler-Bernoulli theory, Timoshenko beam theory and Kirchhoff's plate theory to predict the behavior of nanostructures (Behfar and Naghdabadi 2005; Liew et al. 2006). Since the classical continuum elasticity is a scale-free theory, the use of classical continuum models may be uncertain in the analysis of structural elements in nanoscale such as carbon nanotubes and graphene sheets. There are various modified classical continuum theories which capture size effects such as couple stress theory (Zhou and Li 2001), strain gradient elasticity theory (Fleck and Hutchinson 1997; Akgöz and Civalek 2011), modified couple stress theory (Yang et al. 2002; Akgöz and Civalek 2012) and nonlocal elasticity theory (Eringen and Edelen 1972; Eringen 1983). Among all size-dependent theories, the nonlocal elasticity theory has been commonly applied in the theoretical investigations of structures at small scale (Sudak 2003; Reddy 2007; Reddy and Pang 2008; Heireche et al. 2008; Aydogdu 2009; Farajpour et al. 2011a; Moosavi et al. 2011; Danesh et al. 2012; Mohammadi et al. 2013). To overcome the drawbacks of local elasticity theory, Eringen introduced the nonlocal continuum mechanics in 1972. He modified the classical continuum mechanics for taking into account the nonlocal effects. In this theory, the stress state at a given point depends on the strain states at all points in the domain, while in the local theory, the stress state at any given point depends only on the strain state at that point. Both atomistic simulation results and experimental observations on phonon dispersion have shown the accuracy of this observation (Eringen 1983; Chen et al. 2004).

The applications of graphene sheets in electro-mechanical resonators (Bunch et al. 2007), mass sensors and atomistic dust detectors (Sakhaee-Pour et al. 2008) are recently reported. Furthermore, it has been shown that MnO_2 nanoplates are very promising for wastewater treatment (Ai et al. 2008). Because of these applications, the increasing level of knowledge of vibration and buckling behaviors of nanoplates becomes important for nanoengineering design and manufacture. Duan and Wang (2007) presented an exact closed-form solution for the axisymmetric bending of circular graphene sheets via the nonlocal continuum mechanics and the classical plate theory. Aghababaei and Reddy (2009) developed a nonlocal third-order shear deformation plate theory for the vibration and bending of nanoplates. They presented the results for simply supported boundary conditions. Furthermore, Pradhan and Murmu (2010) employed the nonlocal elasticity theory and differential quadrature method for the buckling analysis of rectangular single-layered graphene sheets under biaxial compression. In addition, they investigated the stability of biaxially compressed orthotropic plates at small scales (Murmu and Pradhan 2009) because it has been reported that the graphene sheets have orthotropic properties (Reddy et al. 2006). They showed that the difference in the buckling load between the isotropic and orthotropic single-layered graphene sheets is relatively larger at lower scale coefficient values. Malekzadeh et al. (2011) investigated the small scale effect on the

thermal buckling of orthotropic arbitrary straight-sided quadrilateral nanoplates embedded in an elastic medium. They found that increasing the elastic medium parameters, the effect of nonlocal parameter on the thermal load ratio decreases. Farajpour et al. (2012) studied the buckling of micro/nanoscale plates under non-uniform compression with the nonlocal elasticity theory. From their results, it can be concluded that in the case of pure in-plane bending, the nonlocal effects are relatively more than other cases (other load factors) and the difference in the effect of small scale between this case and other cases is significant even for larger lengths. In another work, Mohammadi et al. (2013) employed the nonlocal plate theory to analyze the vibration response of circular and annular graphene sheets. They reported that scale effect is less prominent in lower vibration modes and is highly prominent in higher mode numbers. More recently, Asemi et al. (2014) and Asemi and Farajpour (2014) studied the effect of small scale on the thermal buckling and vibration of circular graphene sheets by decoupling the nonlocal elasticity equations in polar coordinates. Mohammadi et al. (2014) presented an exact solution for thermo-mechanical vibration of orthotropic mono-layer graphene sheet embedded in an elastic medium. Moreover, analytical solutions for the nonlocal scaling parameter of zigzag and armchair graphene sheets were obtained and verified using MD simulations by Liang and Han (2014).

All these research works are limited to the linear behavior of graphene sheets. A review of the literature shows that compared to the carbon nanotubes, few research works have been reported on the nonlinear analysis of SLGSs. Recently, Shen et al. (2010) investigated the nonlinear vibration of SLGSs based on the nonlocal plate theory with von Karman geometric nonlinearity. They used MD simulation to determine the nonlocal scaling parameter and anisotropic size-dependent material properties. In their work, numerical results were obtained for six types of armchair and zigzag SLGSs with three different values of aspect ratio. Furthermore, a nonlinear elastic plate model without considering the effect of small scale has been developed for the vibration of multi-layered graphene sheets (Wang et al. 2011). Jomehzadeh et al. (2012) investigated the large amplitude vibration of double-layered graphene sheets embedded in a nonlinear polymer matrix.

In the current work attempt is made to examine the postbuckling response of orthotropic graphene sheets under axial compression. Based on the nonlocal elasticity theory, the small scale effects are taken into account. The geometric nonlinearity is considered with the use of von Karman's strain-displacement relationships. Galerkin method is used to solve the governing equations of single-layered graphene sheet (SLGS) with all edges simply supported. The closed-form solution can be conveniently employed to explore the small scale effects on the postbucking of nanoplates through considering various parameters such as the length of nanoplate, lateral deflection, nonlocal parameter, mode number and aspect ratio. The results show that the nonlocal parameter has prominent effect on the postbuckling behavior of graphene sheets. It is anticipated that the results of the present work would be helpful for designing micro electro-mechanical systems (MEMS) and nano electro-mechanical systems using single-layered graphene sheets.

2 FORMULATION

A rectangular single-layered graphene sheet (SLGS) is shown in Figure 1. SLGS can be modeled as an orthotropic rectangular nonlocal plate. As mentioned in the previous section, recently, many researchers employed the nonlocal plate model for the vibration and buckling analyses of SLGSs.

The graphene sheet's geometric properties are denoted by length, a, width, b and thickness, h. In the present work, the postbuckling of orthotropic rectangular nanoplates under axial compression is investigated (Figure 2). The principal directions of the orthotropic plate are parallel to the sides of the plate. Cartesian coordinate frame with axes x, y and z used for the single layered graphene sheet (SLGS) are shown in Figure 2. The origin of the coordinate system is placed at the lower left corner of the mid-plane of the plate. The x and y axes are also chosen along the length and width of the nanoplate, respectively.

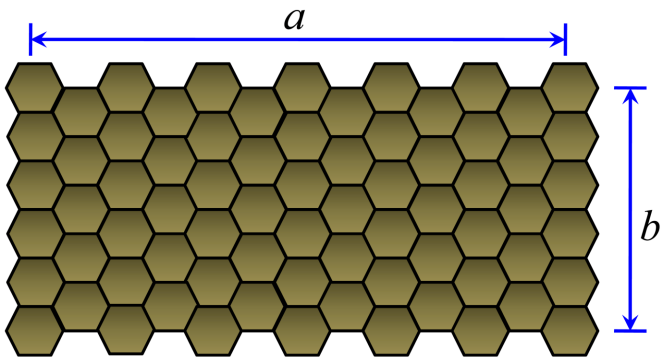

Figure 1 Rectangular single-layered graphene sheet (SLGS).

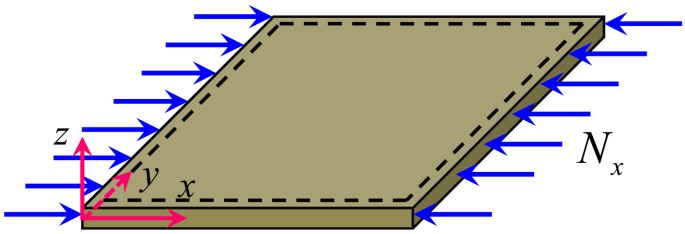

Figure 2 Rectangular nanoplate with all edges simply supported subjected to axial compression.

The following stress resultants and stress couples are used in the present formulation

$$N_{xx} = \int_{-h/2}^{h/2} \sigma_{xx}^{nl}\, dz,\quad N_{yy} = \int_{-h/2}^{h/2} \sigma_{yy}^{nl}\, dz,\quad N_{xy} = \int_{-h/2}^{h/2} \tau_{xy}^{nl}\, dz, \tag{1a}$$

$$M_{xx} = \int_{-h/2}^{h/2} \sigma_{xx}^{nl} z\, dz,\quad M_{yy} = \int_{-h/2}^{h/2} \sigma_{yy}^{nl} z\, dz,\quad M_{xy} = \int_{-h/2}^{h/2} \tau_{xy}^{nl} z\, dz \tag{1b}$$

where σ_x^{nl}, σ_y^{nl} and τ_{xy}^{nl} are the nonlocal normal and shear stresses, respectively. The changes in the mechanical behavior of a nanostructure that are caused by the decrease or increase in its dimensions are called small scale effects or nonlocal effects. Both experimental studies and molecular dy-

namics (MD) simulations have shown that the nonlocal effect (size effect) plays an important role in the mechanical properties of a body at small scale. The traditional local elasticity theory is a scale free theory and thus cannot predict the mechanical characteristics of nanomaterials properly. To overcome the shortcomings of the classical elasticity theory, Eringen modified and extended the local elasticity theory to the nonlocal elasticity problems. He captured the small scale effects by assuming the stress at a point as a function not only of the strain at that point but also a function of the strains at all other points in the domain. Nonlocal theory considers long-range inter-atomic interaction and yields results dependent on the size of a body. The classical elasticity theory is a special case of the nonlocal theory in which stress state at an arbitrary point depends only on the strain state at that point. According to the nonlocal elasticity theory (Eringen, 1983), the basic stress-strain equation for a Hookean solid neglecting the body force is expressed by the following partial-integral constitutive relationship:

$$\sigma_{ij}^{nl} = \iiint_V H(\left|x-x'\right|,\lambda)\sigma_{ij}^{cl}dV \tag{2}$$

The parameters σ_{ij}^{nl} and $\sigma_{ij}^{l}(=C_{ijkl}\varepsilon_{kl})$ are the nonlocal stress and local (macroscopic) stress tensors, respectively. C_{ijkl} and ε_{kl} represent the fourth-order elasticity and strain tensors, respectively. The integration extends over the whole volume of the nanostructure (V). The term $H(\left|x-x'\right|,\lambda)$ is the nonlocal modulus or attenuation function, which depends on the two variables $\left|x-x'\right|$ and λ. The attenuation function incorporates the small scale effects into constitutive equations and has the dimension of $(length)^{-3}$. $\left|x-x'\right|$ represents the distance between x and x' in the Euclidean form. $\lambda(=e_0 l_i/l_e)$ is a material constant that depends on the characteristic length ratio l_i/l_e, where l_i is an internal characteristic length (e.g., lattice parameter, granular distance, distance between C-C bonds) and l_e is an external characteristic length (e.g., crack length, wave length). Choice of the value of parameter e_0 is crucial to calibrate the nonlocal model with experimental results or molecular dynamics (MD) simulation results. Eringen (1983) obtained a value of 0.39 for this parameter by matching the dispersion curves based on atomic models. Wang and Hu (2005) proposed an estimate of the value (e_0) around 0.288 using strain gradient method. Using molecular dynamics and nonlocal Timoshenko beam theory, Duan et al. (2007) reported that the nonlocal scaling effect parameter (e_0) is limited to the range 0 to 19 for the vibration of carbon nanotubes. It is difficult to apply Equation (2) for solving nonlocal elasticity problems. Therefore, the following differential form of Equation (2) is often used (Eringen, 1983):

$$\left(1-l_e^2\lambda^2\nabla^2\right)\sigma^{nl} = \sigma^{cl} \tag{3}$$

where ∇^2 is the Laplacian operator and is given by $\nabla^2(*) = \partial^2(*)/\partial x^2 + \partial^2(*)/\partial y^2$ for a two-dimensional (2D) space. The above stress-strain equation (Equation (3)) is widely used as a basis of

all nonlocal constitutive formulation in the analysis of nanostructures. In particular, the basic stress-strain relationship of orthotropic nanoplates in Cartesian coordinates can be expressed in the following form:

$$\begin{Bmatrix} \sigma_x^{nl} \\ \sigma_y^{nl} \\ \tau_{xy}^{nl} \end{Bmatrix} - (e_0 l_i)^2 \begin{Bmatrix} \sigma_x^{nl} \\ \sigma_y^{nl} \\ \tau_{xy}^{nl} \end{Bmatrix} = \begin{bmatrix} \bar{E}_1 & \bar{E}_{12} & 0 \\ \bar{E}_{21} & \bar{E}_2 & 0 \\ 0 & 0 & \bar{E}_{66} \end{bmatrix} \begin{Bmatrix} \varepsilon_x \\ \varepsilon_y \\ \gamma_{xy} \end{Bmatrix} \tag{4}$$

where

$$\bar{E}_1 = \frac{E_1}{1-\upsilon_{12}\upsilon_{21}}, \quad \bar{E}_2 = \frac{E_2}{1-\upsilon_{12}\upsilon_{21}}, \quad \bar{E}_{12} = \bar{E}_{21} = \frac{\upsilon_{12}E_2}{1-\upsilon_{12}\upsilon_{21}}, \quad \bar{E}_{66} = G_{12} \tag{5}$$

where E_1 and E_2 are Young's modulus, G_{12} is shear modulus, and υ_{12}, υ_{21} are Poisson's ratios, respectively. It should be noted that the shear modulus, Young's modulus and Poisson's ratio are not independent and are related to one another by the following relationships (Behfar and Naghdabadi 2005):

$$\upsilon_{12}E_2 = \upsilon_{21}E_1, \quad G_{12} = \frac{E_1}{2(1+\upsilon_{12})} \tag{6}$$

The postbuckling problem is treated as a geometrically nonlinear problem in the context of Von Karman's assumptions. In this way, the strain-displacement relations at an arbitrary point in the plate can be written as:

$$\begin{aligned} \varepsilon_x &= \varepsilon_x^0 + z\kappa_x, \\ \varepsilon_y &= \varepsilon_y^0 + z\kappa_y, \\ \gamma_{xy} &= \gamma_{xy}^0 + z\kappa_{xy} \end{aligned} \tag{7}$$

The strain components in the plate middle surface are expressed as follows:

$$\varepsilon_x^0 = \frac{\partial u}{\partial x} + \frac{1}{2}\left(\frac{\partial w}{\partial x}\right)^2, \quad \varepsilon_y^0 = \frac{\partial v}{\partial y} + \frac{1}{2}\left(\frac{\partial w}{\partial y}\right)^2, \quad \gamma_{xy}^0 = \frac{\partial u}{\partial y} + \frac{\partial v}{\partial x} + \frac{\partial w}{\partial x}\frac{\partial w}{\partial y} \tag{8}$$

According to the classical plate theory (CPLT), the bending curvatures κ_x, κ_x and twisting curvature κ_{xy} can be written as:

$$\kappa_x = -\frac{\partial^2 w}{\partial x^2}, \quad \kappa_y = -\frac{\partial^2 w}{\partial y^2}, \quad \kappa_{xy} = -2\frac{\partial^2 w}{\partial x \partial y} \tag{9}$$

Eliminating the in-plane components of deformation u and v from Eqation (8), one can obtain the following equation of the compatibility of deformations in the middle surface of the plate:

$$\frac{\partial^2 \varepsilon_x^0}{\partial y^2}+\frac{\partial^2 \varepsilon_y^0}{\partial x^2}-\frac{\partial^2 \gamma_{xy}^0}{\partial x \partial y}=\left(\frac{\partial^2 w}{\partial x \partial y}\right)^2-\frac{\partial^2 w}{\partial x^2}\frac{\partial^2 w}{\partial y^2} \tag{10}$$

The strain-displacement relationships are kinematic equations; therefore, these equations are independent of constitutive equations and can be used to derive the governing equations of nanoplates. Using Equations (1), (4), (5) and (7), the stress resultants can be written in terms of mid-plane strains and curvatures as follows:

$$\begin{Bmatrix} N_x \\ N_y \\ N_{xy} \end{Bmatrix}-(e_0 l_i)^2 \nabla^2 \begin{Bmatrix} N_x \\ N_y \\ N_{xy} \end{Bmatrix}=\begin{bmatrix} B_{11} & B_{12} & 0 \\ B_{21} & B_{22} & 0 \\ 0 & 0 & B_{66} \end{bmatrix}\begin{Bmatrix} \varepsilon_x^0 \\ \varepsilon_y^0 \\ \gamma_{xy}^0 \end{Bmatrix} \tag{11a}$$

$$\begin{Bmatrix} M_x \\ M_y \\ M_{xy} \end{Bmatrix}-(e_0 l_i)^2 \nabla^2 \begin{Bmatrix} M_x \\ M_y \\ M_{xy} \end{Bmatrix}=\begin{bmatrix} D_{11} & D_{12} & 0 \\ D_{21} & D_{22} & 0 \\ 0 & 0 & D_{66} \end{bmatrix}\begin{Bmatrix} \kappa_x \\ \kappa_y \\ \kappa_{xy} \end{Bmatrix} \tag{11b}$$

where

$$B_{11}=\frac{E_1 h}{(1-\upsilon_{12}\upsilon_{21})},\ B_{22}=\frac{E_2 h}{(1-\upsilon_{12}\upsilon_{21})},\ B_{12}=B_{21}=\frac{\upsilon_{12}E_2 h}{(1-\upsilon_{12}\upsilon_{21})},\ B_{66}=G_{12}h \tag{12a}$$

$$D_{11}=\frac{E_1 h^3}{12(1-\upsilon_{12}\upsilon_{21})},\ D_{22}=\frac{E_2 h^3}{12(1-\upsilon_{12}\upsilon_{21})},\ D_{12}=D_{21}=\frac{\upsilon_{12}E_2 h^3}{12(1-\upsilon_{12}\upsilon_{21})},\ D_{66}=\frac{G_{12}h^3}{12} \tag{12b}$$

where $B_{ij}\ (i,j=1,2)$ and $D_{ij}\ (i,j=1,2)$ are called the extensional and bending stiffnesses of the single-layered graphene sheet (SLGS), respectively. B_{66} and D_{66} are also called the shear and torsional rigidities of graphene sheet, respectively. It should be noted that when the nonlocal parameter is set to zero, $(e_0 l_i)=0$, the Equation (11) reduces to that of the classical equation. Using Equations (6), (11a) and (12a), the following matrix relation for the mid-plane strains in terms of the stress resultants can be obtained:

$$\begin{Bmatrix} \varepsilon_x^0 \\ \varepsilon_y^0 \\ \gamma_{xy}^0 \end{Bmatrix}=\frac{1}{h}\begin{bmatrix} 1/E_1 & -\upsilon_{12}/E_1 & 0 \\ -\upsilon_{12}/E_1 & 1/E_2 & 0 \\ 0 & 0 & 1/G_{12} \end{bmatrix}\begin{Bmatrix} L^{nl}N_x \\ L^{nl}N_y \\ L^{nl}N_{xy} \end{Bmatrix} \tag{13}$$

where L^{nl} denotes the nonlocal operator and is given by $L^{nl}(*)=(*)-(e_0 l_i)^2\nabla^2(*)$. Substituting Equation (13) into Equation (10) yields:

$$\frac{1}{h}\left(1-(e_0 l_i)^2\nabla^2\right)\left(\frac{1}{E_1}\frac{\partial^2 N_x}{\partial y^2}+\frac{1}{E_2}\frac{\partial^2 N_y}{\partial x^2}-\frac{\upsilon_{12}}{E_1}\frac{\partial^2 N_x}{\partial x^2}-\frac{\upsilon_{12}}{E_1}\frac{\partial^2 N_y}{\partial y^2}-\frac{1}{G_{12}}\frac{\partial^2 N_{xy}}{\partial x\partial y}\right) = \left(\frac{\partial^2 w}{\partial x\partial y}\right)^2-\frac{\partial^2 w}{\partial x^2}\frac{\partial^2 w}{\partial y^2} \tag{14}$$

Using the equilibrium equations of a differential element of a rectangular plate, the following governing equations can be obtained:

$$\frac{\partial N_x}{\partial x}+\frac{\partial N_{xy}}{\partial y}=0, \tag{15a}$$

$$\frac{\partial N_{xy}}{\partial x}+\frac{\partial N_y}{\partial y}=0, \tag{15b}$$

$$\frac{\partial^2 M_x}{\partial x^2}+2\frac{\partial^2 M_{xy}}{\partial x\partial y}+\frac{\partial^2 M_y}{\partial y^2}+q+\frac{\partial}{\partial x}\left(N_x\frac{\partial w}{\partial x}+N_{xy}\frac{\partial w}{\partial y}\right)+\frac{\partial}{\partial y}\left(N_y\frac{\partial w}{\partial y}+N_{xy}\frac{\partial w}{\partial x}\right)=0 \tag{15c}$$

Here q is the transverse force per unit area. In the present study, it is assumed that the nanoplate is free from any transverse loadings $(q=0)$. Substituting Equations (15a) and (15b) into Equation (15c) and then using Equation (11b), one can obtain the following nonlocal governing differential equation for the stability of graphene sheets under general in-plane loading:

$$D_{11}\frac{\partial^4 w}{\partial x^4}+2(D_{12}+2D_{66})\frac{\partial^4 w}{\partial x^2\partial y^2}+D_{22}\frac{\partial^4 w}{\partial y^4}-\left(1-(e_0 l_i)^2\nabla^2\right)\left(N_x\frac{\partial^2 w}{\partial x^2}+2N_{xy}\frac{\partial^2 w}{\partial x\partial y}+N_y\frac{\partial^2 w}{\partial y^2}\right)=0 \tag{16}$$

It should be noted that in the large deflection analysis of thin plates, unlike the small deformation, the in-plane loads N_x, N_y and N_{xy} depend not only on external loads applied at the mid-plane but also on the stretching of the mid-plane caused by its bending. For convenience and generality, the Airy's stress function Ψ related to in-plane forces can be introduced in the following form:

$$N_x=\frac{\partial^2\Psi}{\partial y^2},\quad N_y=\frac{\partial^2\Psi}{\partial x^2},\quad N_{xy}=-\frac{\partial^2\Psi}{\partial x\partial y} \tag{17}$$

In which $\Psi = \psi h$. It can be easily verified that the above expressions for the in-plane forces satisfy Equations (15a) and (15b). Substituting Equation (17) into Equations (14) and (16), one can obtain the following governing equations:

$$\left(1-(e_0 l_i)^2\nabla^2\right)\left[\frac{1}{E_2}\frac{\partial^4\psi}{\partial x^4}+2\left(\frac{1}{2G_{12}}-\frac{\upsilon_{12}}{E_1}\right)\frac{\partial^4\psi}{\partial x^2\partial y^2}+\frac{1}{E_1}\frac{\partial^4\psi}{\partial y^4}\right]=\left(\frac{\partial^2 w}{\partial x\partial y}\right)^2-\frac{\partial^2 w}{\partial x^2}\frac{\partial^2 w}{\partial y^2} \tag{18}$$

$$\begin{aligned} &D_{11}\frac{\partial^4 w}{\partial x^4}+2(D_{12}+2D_{66})\frac{\partial^4 w}{\partial x^2\partial y^2}+D_{22}\frac{\partial^4 w}{\partial y^4} \\ &-h\left(1-(e_0 l_i)^2\nabla^2\right)\left(\frac{\partial^2\psi}{\partial y^2}\frac{\partial^2 w}{\partial x^2}-2\frac{\partial^2\psi}{\partial x\partial y}\frac{\partial^2 w}{\partial x\partial y}+\frac{\partial^2\psi}{\partial x^2}\frac{\partial^2 w}{\partial y^2}\right)=0 \end{aligned} \tag{19}$$

The Equations (18) and (19) govern the postbuckling of single-layered graphene sheets (SLGSs) under in-plane loading. These fourth-order partial differential equations in terms of the transverse displacement and stress function are coupled and nonlinear. Equations (18) and (19) can be interpreted as the nonlocal compatibility and equilibrium equations, respectively. It should be noted that the traditional local governing differential equations for large deflection of classical plate can be obtained by setting the nonlocal parameter equal to zero ($e_0 l_i = 0$) in the above equations.

In the present study, the postbuckling analysis of SLGSs is studied. Therefore, the van der Waals (vdW) interactions between any two adjacent graphene layers are neglected. However, these interactions must be incorporated into the constitutive equations when the present study extended to the analysis of multi-walled graphene sheets. It is reported in the paper of Reddy et al. (2006) that the graphene sheets possess orthotropic properties. Thus, in the present work we emphasize on orthotropicity of nanoplates.

It can be easily observed that the nonlocal effects enter into the problem through the stress-strain relationship (see Equation (3)). Based on lattice dynamics and molecular dynamics (MD) simulations, Chen et al. (2004) provides an atomic viewpoint to study micro-continuum field theories, including micro-morphic theory, micro-structure theory, micro-polar theory, Cosserat theory, nonlocal theory and couple stress theory, and reported that the nonlocal continuum models are reasonable from a physical point of view.

3 SOLUTION PROCEDURE

3.1 General analytical solution

Consider a rectangular nanoplate with all edges simply supported, as shown in Figure 2. The plate is subjected to the uniformly distributed compressive forces in x direction (N_x). An approximate expression for the transverse deflection of the middle surface of the nanoplate can be written in the following form:

$$w = W\sin(\alpha x)\sin(\beta y) \tag{20}$$

In the above expression, $\alpha = n\pi/a$ and $\beta = m\pi/b$. In previous section, in order to investigate the postbuckling behavior of single-layered graphene sheet with constant thickness, two governing differential equations are derived based on von Karman's assumptions and nonlocal continuum mechanics. Substituting Equation (20) into the compatibility equation (18) leads to

$$\left(1-(e_0 l_i)^2\nabla^2\right)\left[\frac{1}{E_2}\frac{\partial^4\psi}{\partial x^4}+2\left(\frac{1}{2G_{12}}-\frac{\upsilon_{12}}{E_1}\right)\frac{\partial^4\psi}{\partial x^2\partial y^2}+\frac{1}{E_1}\frac{\partial^4\psi}{\partial y^4}\right]=\frac{1}{2}W^2\alpha^2\beta^2\left(\cos(2\alpha x)+\cos(2\beta y)\right) \tag{21}$$

A particular solution of the above nonhomogeneous differential equation can be taken as follows:

$$\psi_p = A_1\cos(2\alpha x)+A_2\cos(2\beta y) \tag{22}$$

where A_1 and A_2 are two unknown coefficients which can be obtained by substituting Equation (22) into Equation (21) and then comparing the left- and right-hand sides of Equation (21). Therefore, one can obtain the following expressions:

$$\begin{aligned} A_1 &= \frac{E_2W^2}{32}\left(\frac{ma}{nb}\right)^2\left(\frac{1}{1+4n^2\pi^2\left(e_0l_i/a\right)^2}\right), \\ A_2 &= \frac{E_1W^2}{32}\left(\frac{nb}{ma}\right)^2\left(\frac{1}{1+4m^2\pi^2\left(e_0l_i/b\right)^2}\right) \end{aligned} \tag{23}$$

From these relationships, it can be easily seen that the nonlocal parameter ($e_0 l_i$) appears in the coefficients of particular solution of Airy's stress function. It is assumed that the edge supports do not prevent the in-plane movements of the SLGS in the y direction. The homogeneous solution of the Equation (21) is taken in the form

$$\psi_h = -\frac{P_x y^2}{2h} \tag{24}$$

According to the theory of differential equations, the general solution of nonlocal compatibility Equation (21) is the sum of the homogeneous solution and the particular solution. Consequently, the general solution is as follows:

$$\psi = -\frac{P_x y^2}{2h}+\frac{E_2\left(maW\right)^2}{32\left(nb\right)^2\left[1+4n^2\pi^2\left(e_0l_i/a\right)^2\right]}\cos(2\alpha x)+\frac{E_1\left(nbW\right)^2}{32\left(ma\right)^2\left[1+4m^2\pi^2\left(e_0l_i/b\right)^2\right]}\cos(2\beta y) \tag{25}$$

In-plane force resultants in the middle surface of the nanoplate are

$$\begin{aligned} N_x &= -P_x - \frac{E_1 h\left(n\pi W\right)^2}{8a^2\left[1+4m^2\pi^2\left(e_0 l_i/b\right)^2\right]}\cos\left(2\beta y\right), \\ N_y &= -\frac{E_2 h\left(m\pi W\right)^2}{8b^2\left[1+4n^2\pi^2\left(e_0 l_i/a\right)^2\right]}\cos\left(2\alpha x\right), \quad N_{xy}=0 \end{aligned} \tag{26}$$

Note that the in-plane shear force is zero. In addition, prior to buckling of the nanoplate, the uniformly distributed compressive force N_x acts on the two opposite edges $x=0$ and $x=a$; however, subsequent to buckling the distribution of normal in-plane force along the loaded edges becomes progressively nonlinear. Compressive force increases more intensively in the neighborhood of the plate edges ($y=0$ and $y=b$).

3.2 Solutions by Galerkin method

In this section, Galerkin method is employed for the solution of the governing equations. The Galerkin method is a powerful and efficient numerical technique to solve the differential equations. Since this numerical method provides simple formulation and low computational cost, it has been widely used for the analysis of mechanical behavior of the structural elements at large scale, such as static, dynamic and stability problems. The Galerkin method was used by Romeo and Frulla (1997) to study the postbuckling behavior of stiffened composite panels under biaxial compressive load. Saadatpour and Azhari (1998) used Galerkin technique for static analysis of simply supported plates of arbitrary quadrilateral shape. Furthermore, the small-deflection stability analysis of various quadrilateral nanoplates, such as skew, rhombic, and trapezoidal nanoplates, was carried out on the basis of the Galerkin method (Babaei and Shahidi 2010). Using the general procedure of the method yields the following:

$$\int_0^b\int_0^a J\left(x,y\right)\sin\left(\alpha x\right)\sin\left(\beta y\right)dxdy = 0 \tag{27}$$

where

$$\begin{aligned} J\left(x,y\right) \equiv{}& D_{11}\frac{\partial^4 w}{\partial x^4} + 2(D_{12}+2D_{66})\frac{\partial^4 w}{\partial x^2\partial y^2} + D_{22}\frac{\partial^4 w}{\partial y^4} \\ &-h\left(1-(e_0 l_i)^2\nabla^2\right)\left(\frac{\partial^2\psi}{\partial y^2}\frac{\partial^2 w}{\partial x^2} - 2\frac{\partial^2\psi}{\partial x\partial y}\frac{\partial^2 w}{\partial x\partial y} + \frac{\partial^2\psi}{\partial x^2}\frac{\partial^2 w}{\partial y^2}\right) \end{aligned} \tag{28}$$

Note that a set of functions 1, $\sin\left(\pi x\right)$, $\sin\left(2\pi x\right)$, ..., $\sin\left(k\pi x\right)$, ... is mutually orthogonal in the interval $0\le x\le 2\pi$. Substituting for deflection and stress function (w and ψ) from Equations (20)

and (25) into (28) and then performing the corresponding operations of differentiations, the function $J(x,y)$ can be expressed as:

$$\begin{aligned} J(x,y) = \left[\eta_1 + \eta_2\left(1+(e_0 l_i)^2\left[\alpha^2+\beta^2\right]\right)\right]\sin(\alpha x)\sin(\beta y) - \eta_3\left(1+(e_0 l_i)^2\left[\alpha^2+9\beta^2\right]\right)\sin(\alpha x)\sin(3\beta y) \\ -\eta_4\left(1+(e_0 l_i)^2\left[9\alpha^2+\beta^2\right]\right)\sin(3\alpha x)\sin(\beta y) \end{aligned} \tag{29}$$

where

$$\begin{aligned} \eta_1 &= W\left(D_{11}\alpha^4 + 2(D_{12}+2D_{66})\alpha^2\beta^2 + D_{22}\beta^4\right), \\ \eta_2 &= -P_x W\alpha^2 + \frac{hW^3}{16}\left(\frac{E_1\alpha^4}{\left[1+4\beta^2\left(e_0 l_i\right)^2\right]} + \frac{E_2\beta^4}{\left[1+4\alpha^2\left(e_0 l_i\right)^2\right]}\right), \\ \eta_3 &= \frac{E_1 h\alpha^4 W^3}{16\left[1+4\beta^2\left(e_0 l_i\right)^2\right]}, \quad \eta_4 = \frac{E_2 h\beta^4 W^3}{16\left[1+4\alpha^2\left(e_0 l_i\right)^2\right]} \end{aligned} \tag{30}$$

Using Equations (29), (30) and (27) and assuming that $W \neq 0$, yields the following equation for the postbuckling of orthotropic nanoplats:

$$\begin{aligned} \bar{P}_x = \frac{1}{1+\lambda^2\pi^2\left(n^2+m^2\chi^2\right)}\Bigg\{ \pi^2 m^2\left[\left(\frac{n}{m}\right)^2 + 2\chi^2 Q_{12} + \chi^4 Q_{22}\left(\frac{m}{n}\right)^2\right] \\ + \frac{3\pi^2(1-\upsilon_{12}\upsilon_{21})\mu^2}{4n^2}\left(\frac{n^4}{1+4\chi^2\left(m\pi\lambda\right)^2} + \frac{\chi^4 m^4}{1+4\left(n\pi\lambda\right)^2}Q_{22}\right)\left(1+\pi^2\lambda^2\left[n^2+m^2\chi^2\right]\right)\Bigg\} \end{aligned} \tag{31}$$

In the above equation, the non-dimensional parameters are defined as follows:

$$\bar{P}_x = \frac{P_x a^2}{D_{11}},\ \lambda = \frac{e_0 l_i}{a},\ \chi = \frac{a}{b},\ \mu = \frac{W}{h},\ Q_{22} = \frac{D_{22}}{D_{11}},\ Q_{12} = \frac{D_{12}+2D_{66}}{D_{11}} \tag{32}$$

Inserting D_{11}, D_{22}, D_{66} and D_{12} from Equation (12b) into the above expressions for Q_{22} and Q_{12} and using Equation (6), leads to the following expressions:

$$Q_{12} = \frac{1+\upsilon_{21}}{1+\upsilon_{12}},\ Q_{22} = \frac{E_2}{E_1} \tag{33}$$

It should be noted that the first term on the right-hand side of Equation (31) indicates the critical force for the linear stability analysis of SLGSs. Consequently, it is obvious that the nonlinear buckling load of the nanoplate is greater than the linear buckling load. Furthermore, the classical closed-form solution for the postbuckling of local plate under axial compression can be obtained by setting the nonlocal parameter equal to zero ($\lambda = 0$) in the Equation (31). In other words, the scale coefficient (nonlocal parameter) transforms the traditional equations of classical continuum mechanics into the corresponding governing equations of nonlocal continuum mechanics. This parameter ($e_0 l_i$) is taken into the constitutive equations simply as a material constant.

4 RESULTS AND DISCUSSION

4.1 Validation of present results

To validate the computed results, the linear nonlocal buckling loads of a square SLGS under biaxial compression are compared with those of molecular dynamic (MD) simulations obtained by Ansari and Rouhi (2012). The material properties of nanoplate are taken as $E_1 = E_2 = 1\ TPa$ and $\upsilon_{21} = \upsilon_{12} = 0.16$ (Ansari and Rouhi 2012). A value of $h = 0.34$ nm is assumed for the thickness of SLGS. Figure 3 shows the critical buckling loads of SLGS versus the variation of nanoplate's length for different values of nonlocal parameter $(e_0 l_i)^2$. It is found that the present results are in good agreement with those of MD simulations for $(e_0 l_i)^2 = 1.85\ \text{nm}^2$. As another example, the present results are compared with the nonlocal results of a square SLGS with simply supported boundary conditions as reported by Pradhan and Murmu (2010). The comparison is shown in Figure 4. The nanoplate is subjected to uniaxial loading. The length of the plate varies from 5 to 45 nm. It is assumed that the material of the SLGS is homogeneous and isotropic. From this figure, it is clearly seen that the present results exactly match with those obtained by Pradhan and Murmu (2010).

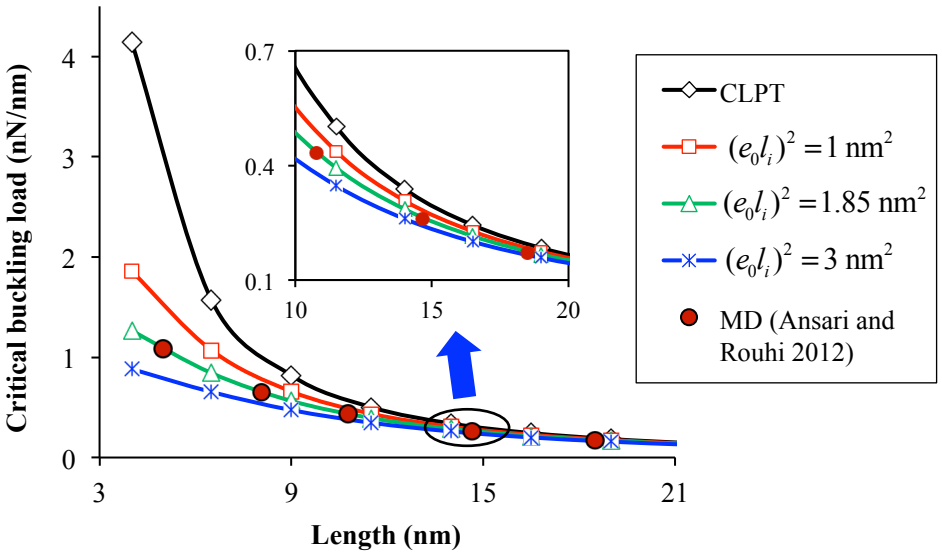

Figure 3 Comparison of present results with those of MD simulation (Ansari and Rouhi 2012) for isotropic SLGS

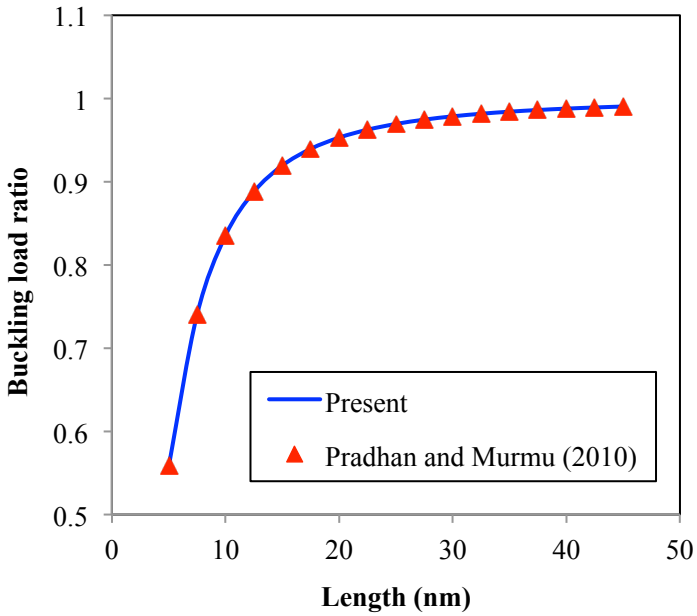

Figure 4 Comparison of present results with those obtained by Pradhan and Murmu (2010).

4.2 Nonlocal effects on the postbuckling of SLGS

In order to illustrate the small scale effects on the postbuckling response of single-layered graphene sheets, the nonlocal load ratio is defined as follows:

$$Nonlocal\ load\ ratio = \frac{Nonlocal\ postbuckling\ load\ (e_0 l_i \neq 0)}{Local\ postbuckling\ load\ (e_0 l_i = 0)} \tag{34}$$

Figure 5 shows the variation of nonlocal load ratio with the non-dimensional lateral deflection for various values of nonlocal parameter ($e_0 l_i$). The results are computed using Equation (31). The side length of square SLGS is taken as 10 nm. The value of nonlocal parameter is chosen in the range of 0-2 nm. The reason for taking these values is that Wang and Wang (2007) reported that the scale factor ($e_0 l_i$) of a single-wall carbon nanotube (SWCNT) must be smaller than 2.0 nm. They also presented the constitutive relations of nonlocal elasticity theory for the application in the analysis of carbon nanotubes (CNTs) when modeled as Euler–Bernoulli beams, Timoshenko beams or as cylindrical shells. Recently, many researchers used these values for the nonlocal parameter in the analysis of graphene sheets (Duan and Wang 2007; Pradhan and Murmu 2010; Farajpour 2011b). For numerical results, the following Young's modulus and Poisson's ratios are used throughout the investigation (Behfar and Naghdabadi 2005):

$$E_1 = 1765\ Gpa,\ E_2 = 1588\ Gpa \text{ and } \upsilon_{12} = 0.3,\ \upsilon_{21} = 0.27$$

From Figure 5, it is found that the critical postbuckling load calculated using nonlocal theory, are always smaller than the critical postbuckling load calculated using classical theory for all nonlocal parameters (nonlocal load ratio ≤ 1). Furthermore, the amounts of nonlocal load ratios gradually decrease by increasing the lateral deflection from 0 to 5. This means that as the ratio of deflection to the plate thickness increases the influence of small length scale increases. This increase in the nonlocal effects is more intensive for large values of nonlocal parameter. In fact, the nonlocal load ratio remains unchanged for small nonlocal parameter and large deflection. The nonlocal load ratio decreases with increase in nonlocal factor from 0 to 2 nm at a constant lateral deflection. This implies that the stiffness of structure decreases with the increase in nonlocal parameter.

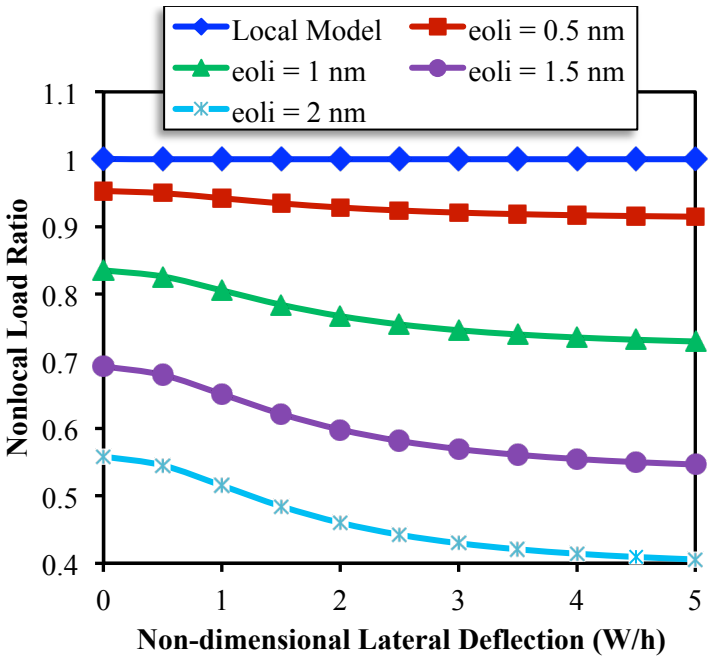

Figure 5 Change of nonlocal load ratio with non-dimensional lateral deflection for different nonlocal parameters (side length = 10 nm).

The variation of nonlocal load ratio with the side length is plotted in Figure 6 for a square nanoplate. A value of 3 is taken for the non-dimensional lateral deflection. Various nonlocal factors are considered for the square SLGS in this figure. It is found that as the side length of the nanoplates increases the nonlocal load ratio increases and the curves become flat. An evident reason of this phenomenon is that the influence of small length scale reduces with the increase of nanoplate's length. The size effects are lost after a certain length for each nonlocal parameter. Further, it is observed that the length, in which the nonlocal effects can be ignored, depends on the nonlocal parameter. The value of this length increases with increase of nonlocal parameter. For example, in the case of $e_0 l_i = 1$ nm, the plate is released from size effects when side length is greater than about 36 nm, while the approximate value for the length is 44 nm for $e_0 l_i = 1.5$ nm.

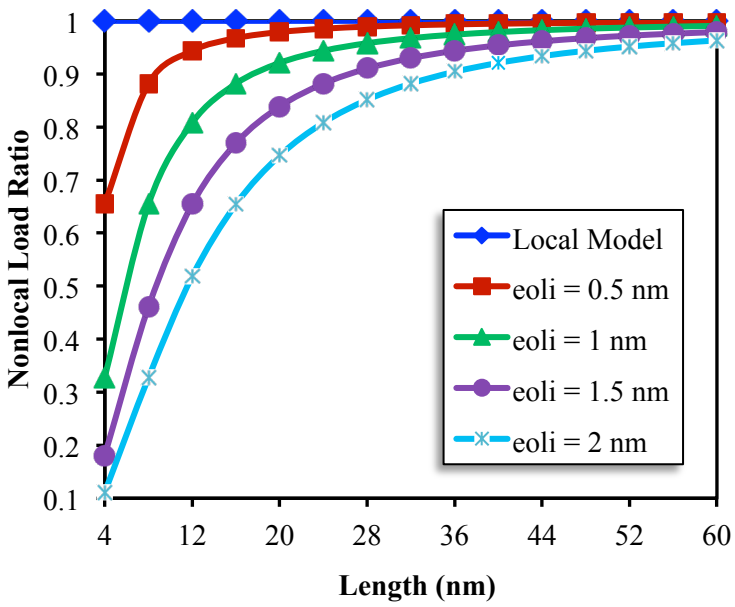

Figure 6 Change of nonlocal load ratio with the length of square graphene sheet for various nonlocal parameters (W/h = 3).

4.3 Effect of higher modes on the postbuckling of SLGS

To show the effect of small scale on higher postbuckling modes, nonlocal load ratio versus the variation of non-dimensional lateral deflection are plotted for first five mode numbers (*m=1*, *n=1-5*) and three values of nonlocal factors, $e_0 l_i = 0.7,\ 1.4$ and 2 nm, in Figures 7, 8 and 9, respectively. The length and aspect ratio of the nanoplate are assumed as $a = 10$ nm and $a/b = 1$, respectively. It is evident from these figures that as the lateral deflection of nanoplate increases the nonlocal load ratio decreases for the first mode number ($n = 1$). However, the load ratio approximately remains constant with increase in lateral deflection for the second mode number ($n = 2$). In addition, lateral deflection has an increasing effect on the load ratio at higher modes ($n \geq 3$). It is also found that all load ratio curves close to each other by increasing deflection to thickness ratio. The gap between each two curves (except for first mode) diminishes after a certain lateral deflection ($W/h \geq 3.5$). In other words, when graphene sheets with same nonlocal parameter are considered at higher modes ($n \geq 2$) and large lateral deflection ($W/h \geq 3.5$), the nonlocal load ratio is independent of mode number. In addition, the effect of small length scale is higher for higher modes ($W/h \leq 3.5$). This phenomenon is because of small wavelength effect for higher modes. At smaller wavelengths (higher mode numbers), the interaction between atoms increases and it causes an increase in the small scale effects. When Figure 7 is compared with Figures 8 and 9, one can easily observed that all curves shift down by increasing the nonlocal parameter. This is obvious because the nonlocal effect increases with increase of nonlocal parameter.

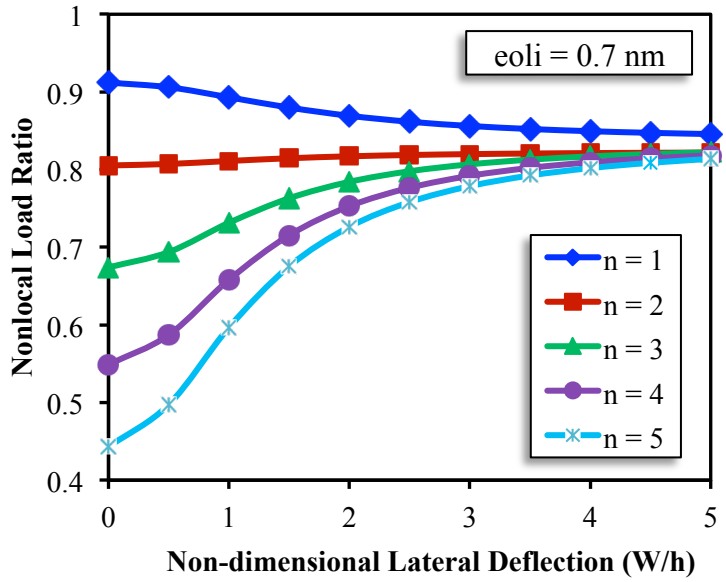

Figure 7 Change of nonlocal load ratio with non-dimensional lateral deflection for different mode numbers (nonlocal parameter = 0.7 nm).

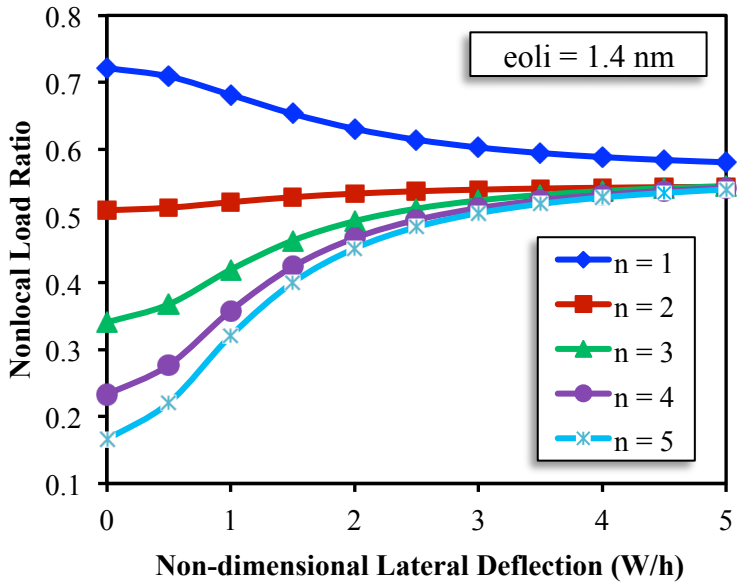

Figure 8 Change of nonlocal load ratio with non-dimensional lateral deflection for different mode numbers (nonlocal parameter = 1.4 nm).

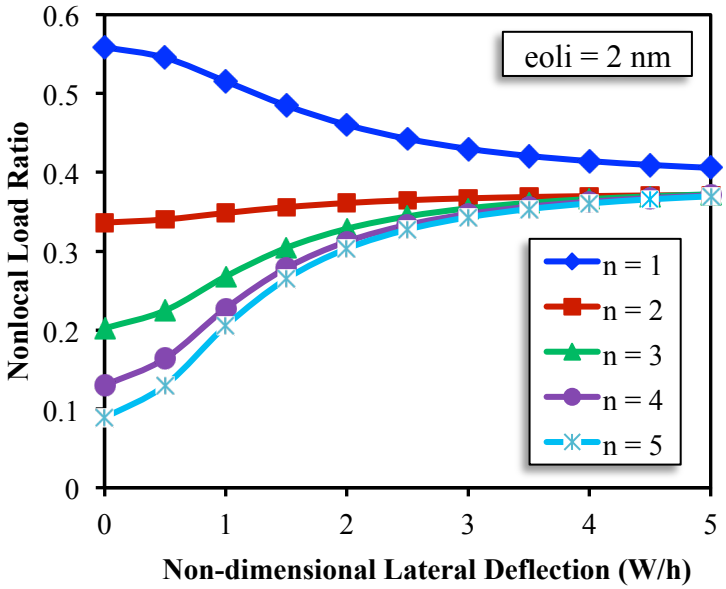

Figure 9 Change of nonlocal load ratio with non-dimensional lateral deflection for different mode numbers (nonlocal parameter = 2 nm).

4.4 Effect of aspect ratio on the postbuckling of SLGS

To see the effect of aspect ratio on nonlinear buckling response of nanoplates, the change of nonlocal load ratio with aspect ratio ($\chi = a/b$) is plotted for various non-dimensional lateral deflections ($\mu = W/h$ = 0, 1, 2, 3, 4), as shown in Figure 10. The ratio of the length to the width (aspect ratio) is considered in the range of 0.1 to 1.5. Lower aspect ratio would represent a strip-type nanoplate (nanoribbon). The value of $a = 10$ nm is taken for the length of nanoplate. $e_0 l_i$ is chosen as 0.7 nm. From Figure 10, it is clearly seen that the load ratio decreases with increase of aspect ratio from 0.1 to 1.5 and it leads the small scale effects increase. This is because of decreasing the width of SLGS with increase of aspect ratio at a certain side length which leads to an increase in the nonlocal effects. It is interesting to note that all curves pass through a point ($\chi \approx 0.52$). Before this point, namely, for the nanoribbon with the aspect ratio in the range of 0.1-0.52, the nonlocal effects are more pronounced for the small deflection compared with the large deflection of the nanoplate. However, after the point ($\chi \geq 0.52$) nonlocal effects increase with increasing non-dimensional lateral deflection from 0 to 4. Similar results could be observed from Figures 11 and 12, in which the nonlocal parameter is taken as $e_0 l_i = 1.4$ and 2 nm, respectively. Similar to the results discussed in the foregoing subsection, all curves shift down by increasing the nonlocal parameter.

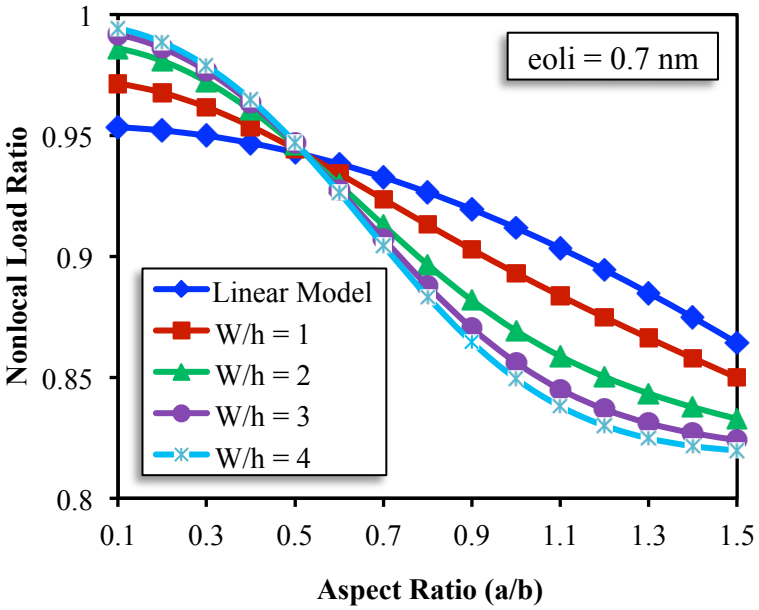

Figure 10 Change of nonlocal load ratio with the aspect ratio of graphene sheet for different lateral deflections (nonlocal parameter = 0.7 nm).

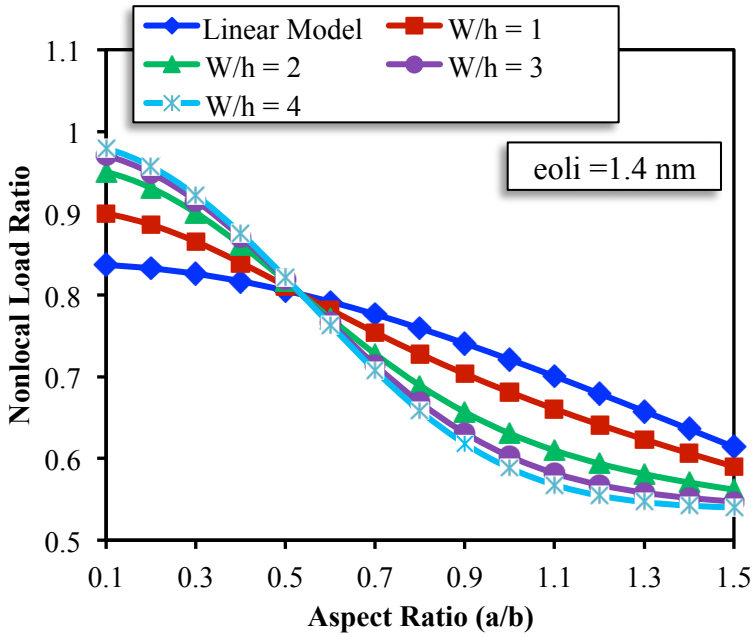

Figure 11 Change of nonlocal load ratio with the aspect ratio of graphene sheet for different lateral deflections (nonlocal parameter = 1.4 nm).

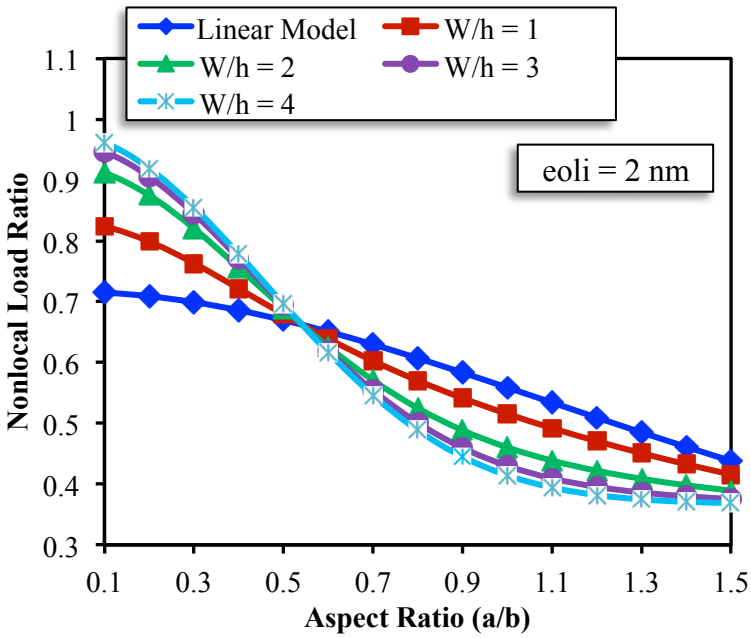

Figure 12 Change of nonlocal load ratio with the aspect ratio of graphene sheet for different lateral deflections (nonlocal parameter = 2 nm).

4.5 Comparison in critical loads obtained from linear and nonlinear theories

Critical axial forces obtained from nonlinear theory ($W/h \neq 0$) are compared with those obtained from linear theory ($W/h \neq 0$). The percentage difference in critical force calculated using linear and nonlinear theories in single-layered graphene sheet has been defined as follows:

$$Percentage\ difference = \frac{\bar{P}_x\big|_{\mu\neq 0} - \bar{P}_x\big|_{\mu=0}}{\bar{P}_x\big|_{\mu=0}} \tag{35}$$

This percentage difference in critical loads versus non-dimensional lateral deflection for various nonlocal parameters and mode numbers are plotted in Figures 13 and 14, respectively. The side length of square SLGS is assumed to be 5 nm. The results in Figure 13 reveal that the percentage difference in critical loads between linear and nonlinear theories is significantly larger for larger values of W/h ratios. So, when lateral deflection is comparable to the thickness of the graphene sheet, nonlinear plate theory yields more accurate results. It is interesting to note that the difference decreases with increasing the nonlocal parameter. Figure 14 depicts the percentage difference of square nanoplates for the first five mode numbers with the lateral deflection. The value of nonlocal parameter is taken as $e_0 l_i$ =2 nm. It can be observed that the nonlinearity related to the midplane extension is quite noticeable and profound for the higher postbuckling modes.

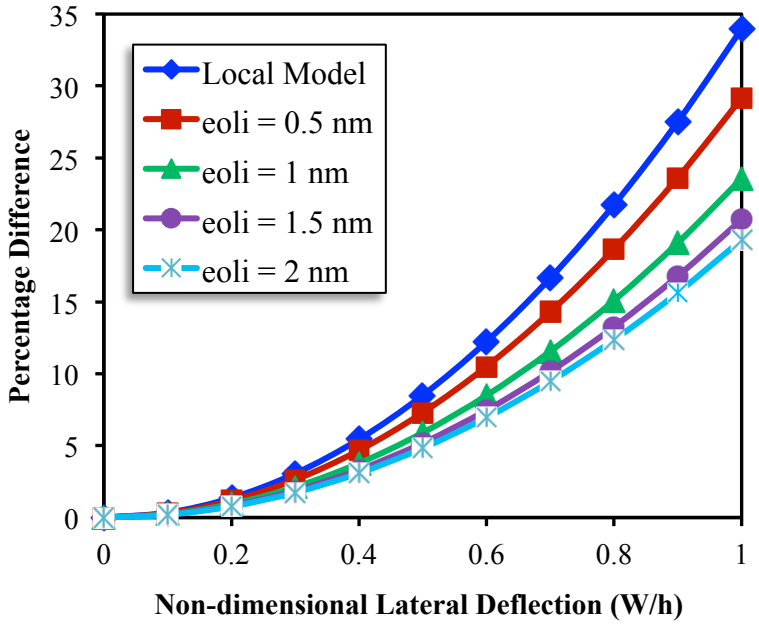

Figure 13 Percentage difference in critical load between linear and nonlinear nonlocal plate theories versus W/h ratio for different nonlocal parameters (side length = 5 nm).

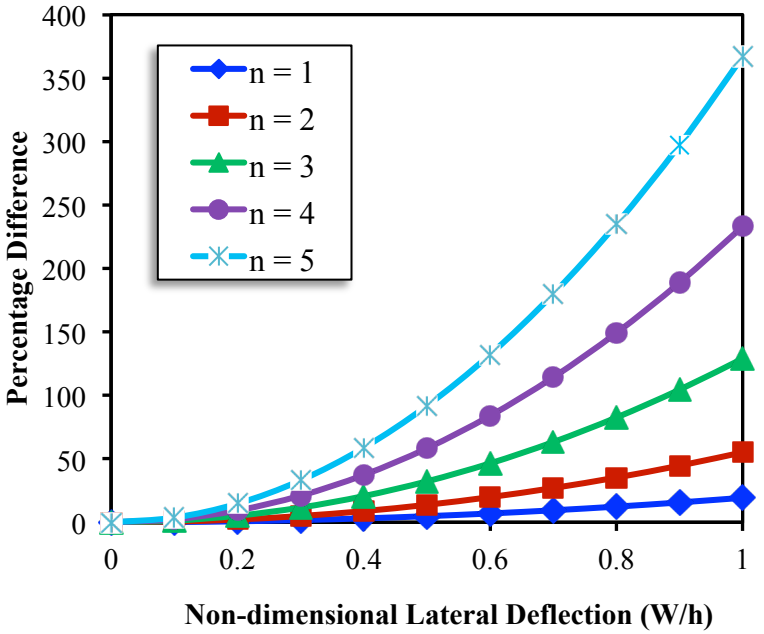

Figure 14 Percentage difference in critical load between linear and nonlinear nonlocal plate theories versus W/h ratio for different mode numbers (side length = 5 nm, eoli = 2 nm).

5 CONCLUSIONS

This manuscript presents closed-form solutions for the postbuckling behavior of single-layered graphene sheet subjected to axial compression based on the nonlocal continuum mechanics. The geometrical nonlinearity is modeled with the use of von Karman's assumptions. Galerkin method is applied to solve the governing nonlocal equations for postbuckling response. Results for orthotropic rectangular nanoplates with all edges simply supported are presented. From the results following conclusions are noticeable:

- The nonlocal effect reduces with the increase of nanoplate's length and vanishes after a certain length for each nonlocal parameter.
- Higher postbuckling mode is more significant at smaller lateral deflection.
- Small scale effects increase by increasing the lateral deflection of nanoplate for the first mode number ($n=1$).
- Nonlocal effects are approximately independent of the lateral deflection for the second mode number ($n=2$).
- The lateral deflection has a decreasing effect on the size effects at higher modes ($n>2$).
- The effect of small length scale is higher for higher modes.
- Nonlocal effects are more prominent for the small deflection compared with the large deflection of nanoribbons with the aspect ratio in the range of 0.1-0.52.
- The percentage difference in critical loads between linear and nonlinear theories decreases with increasing the nonlocal parameter.
- The nonlinearity caused by the extension of middle surface is much more important at higher postbuckling modes.

References

Aghababaei, R., Reddy, J.N. (2009). Nonlocal third-order shear deformation plate theory with application to bending and vibration of plates, J Sound Vib 326: 277-89.

Ai, Z., Zhang, L., Kong, F., Liu, H., Xing, W., Qiu, J. (2008). Microwave-assisted green synthesis of MnO_2 nanoplates with environmental catalytic activity, Mater Chem Phys 111: 162–167.

Akgöz, B., Civalek, Ö. (2011). Application of strain gradient elasticity theory for buckling analysis of protein microtubules, Current Applied Physics 11: 1133-1138.

Akgöz, B., Civalek, Ö. (2012). Free vibration analysis for single-layered graphene sheets in an elastic matrix via modified couple stress theory, Materials & Design 42: 164-171.

Ansari, R., Rouhi, H. (2012). Explicit analytical expressions for the critical buckling stresses in a monolayer graphene sheet based on nonlocal elasticity, Solid State Commun 152: 56-59.

Asemi, S.R., Farajpour, A., Borghei, M., Hassani, A.H. (2014). Thermal effects on the stability of circular graphene sheets via nonlocal continuum mechanics, Lat Am J Solids Struct 11: 704-724.

Asemi, S.R., Farajpour, A. (2014). Decoupling the nonlocal elasticity equations for thermo-mechanical vibration of circular graphene sheets including surface effects, Physica E, doi: http://dx.doi.org/10.1016/j.physe.2014.02.002.

Aydogdu, M. (2009). Axial vibration of the nanorods with nonlocal continuum rod model, Physica E 41: 861-864.

Babaei, H., Shahidi, A.R. (2010). Small-scale effects on the buckling of quadrilateral nanoplates based on nonlocal elasticity theory using the Galerkin method, Arch Appl Mech 81: 1051–1062.

Behfar, K., Naghdabadi, R. (2005). Nanoscale vibrational analysis of a multi-layered graphene sheet embedded in an elastic medium, Compos Sci Tech 65: 1159-1164.

Bunch, J.S., van der Zande, A.M., Verbridge, S.S., Frank, I.W., Tanenbsum, D.M., Parpia, J.M., Craighead, H.G., McEuen, P.L. (2007). Electromechanical resonators from graphene sheets, Science 315: 490-3.

Chen, Y., Lee, J.D., Eskandarian, A. (2004) Atomistic view point of the applicability of micro-continuum theories, Int J Solids Struct 41: 2085-2097.

Danesh, M., Farajpour, A., Mohammadi, M. (2012). Axial vibration analysis of a tapered nanorod based on nonlocal elasticity theory and differential quadrature method, Mech Res Commun 39: 23-27.

Duan, W.H., Wang, C.M. (2007). Exact solutions for axisymmetric bending of micro/nanoscale circular plates based on nonlocal plate theory, Nanotechnology 18: 385704.

Duan, W.H., Wang, C.M., Zhang, Y.Y. (2007). Calibration of nonlocal scaling effect parameter for free vibration of carbon nanotubes by molecular dynamics, J Appl Phys 101: 024305.

Eringen, A.C., Edelen, D.G.B. (1972). On nonlocal elasticity, Int J Eng Sci 10: 233-248.

Eringen, A.C. (1983). On differential equations of nonlocal elasticity and solutions of screw dislocation and surface waves, J Appl Phys 54: 4703-4711.

Farajpour A., Mohammadi M., Shahidi A.R., Mahzoon M. (2011a). Axisymmetric buckling of the circular graphene sheets with the nonlocal continuum plate model. Physica E 43: 1820 –1825.

Farajpour, A., Danesh, M., Mohammadi, M. (2011b). Buckling analysis of variable thickness nanoplates using nonlocal continuum mechanics, Physica E 44: 719-727.

Farajpour, A., Shahidi, A.R., Mohammadi, M., Mahzoon, M. (2012). Buckling of orthotropic micro/nanoscale plates under linearly varying in-plane load via nonlocal continuum mechanics, Compos Struct 94: 1605-1615.

Fleck, N.A., Hutchinson, J.W. (1997) Strain gradient plasticity, Adv Appl Mech 33: 296-358.

Craighead H.G. (2000). Nanoelectromechanical systems, Science 290: 1532-1535.

Heireche, H., Tounsi, A., Benzair, A., Maachou, M., Adda Bedia, E.A. (2008). Sound wave propagation in single-walled carbon nanotubes using nonlocal elasticity, Physica E 40: 2791-2799.

Iijima, S. (1991). Helical microtubules of graphitic carbon, Nature 354: 56-58.

Jomehzadeh, E., Saidi, A.R., Pugno, N.M. (2012). Large amplitude vibration of a bilayer graphene embedded in a nonlinear polymer matrix, Physica E 44: 1973-1982.

Liang, Y., Han, Q. (2014). Prediction of the nonlocal scaling parameter for graphene sheets, Eur. J. Mech. A/Solids 45: 153-160.

Liew, K.M., He, X.Q., Kitipornchai, S. (2006). Predicting nanovibration of multi-layered graphene sheets embedded in an elastic matrix, Acta Mater 54: 4229-4236.

Li, M., Tang, H.X., Roukes, M.L. (2007). Ultra-sensitive NEMS-based cantilevers for sensing, scanned probe and very high-frequency applications, Nature Nanotechnology 2: 114-120.

Malekzadeh, P., Setoodeh, A.R., Alibeygi Beni, A. (2011b). Small scale effect on the thermal buckling of orthotropic arbitrary straight-sided quadrilateral nanoplates embedded in an elastic medium, Compos Struct 93: 2083–2089.

Miller, R.E., Shenoy, V.B. (2000). Size-dependent elastic properties of nanosized structural elements, Nanotechnology 11: 139–47.

Mohammadi, M., Ghayour, M., Farajpour A. (2013). Free transverse vibration analysis of circular and annular graphene sheets with various boundary conditions using the nonlocal continuum plate model, Composites Part B 45: 32-42.

Mohammadi, M., Moradi, A., Ghayour, M., Farajpour, A. (2014). Exact solution for thermo-mechanical vibration of orthotropic mono-layer graphene sheet embedded in an elastic medium, Lat Am J Solids Struct 11: 437-458.

Moosavi, H., Mohammadi, M., Farajpour, A., Shahidi, S.H. (2011). Vibration analysis of nanorings using nonlocal continuum mechanics and shear deformable ring theory, Physica E 44: 135-140.

Murmu, T., Adhikari, S. (2010). Nonlocal effects in the longitudinal vibration of double-nanorod systems, Physica E 43: 415-422.

Murmu, T., Pradhan, S.C. (2009). Buckling of biaxially compressed orthotropic plates at small scales, Mech Res Commun 36: 933–938.

Pradhan, S.C., Murmu, T. (2010). Small scale effect on the buckling analysis of single-layered graphene sheet embedded in an elastic medium based on nonlocal plate theory, Physica E 42: 1293-1301.

Reddy, C.D., Rajendran, S., Liew, K.M. (2006). Equilibrium configuration and continuum elastic properties of finite sized graphene, Nanotechnology 17: 864–870.

Reddy, J.N. (2007). Nonlocal theories for bending, buckling and vibration of beams, Int J Eng Sci 45: 288-307.

Reddy, J.N., Pang, S.D. (2008). Nonlocal continuum theories of beams for the analysis of carbon nanotubes, J Appl Phys 103: 023511.

Romeo, G., Frulla, G. (1997). Post-buckling behaviour of graphite/epoxy stiffened panels with initial imperfections subjected to eccentric biaxial compression loading, Int J Non-Linear Mech 3: 1017–1033.

Saadatpour, M.M., Azhari, M. (1998). The Galerkin method for static analysis of simply supported plates of general shape, Computers and Structures 69: 1-9.

Sakhaee-Pour, A., Ahmadian, M.T., Vafai, A. (2008). Applications of single-layered graphene sheets as mass sensors and atomistic dust detectors, Solid State Commun 145: 168-172.

Saremi, F., Haeri, H.H., Hasani, A.H., Mansouri, N. (2008). Adsorption of Carbon Monoxide on a (6, 6) Armchair Carbon Nanotube: Ab initio Study, J Phys Theor Chem IAU 4(4): 235-238.

Shen L., Shen H.S., Zhang C.L. (2010). Nonlocal plate model for nonlinear vibration of single layer graphene sheets in thermal environments, Comput Mater Sci 48: 680-685.

Sudak, L.J. (2003) Column buckling of multi-walled carbon nanotubes using nonlocal continuum mechanics, J Appl Phys 94: 7281-7287.

Wang, L.F., Hu, H.Y. (2005). Flexural wave propagation in single-walled carbon nanotubes, Phys Rev B 71: 195412.

Wang, Q., Wang, C.M. (2007). The constitutive relation and small scale parameter of nonlocal continuum mechanics for modelling carbon nanotubes, Nanotechnology 18: 075702.

Wang, J., He, X., Kitipornchai, S., Zhang, H. (2011). Geometrical nonlinear free vibration of multi-layered graphene sheets, J Phys D: Appl Phys 44: 135401.

Yang, F., Chong, A.C.M., Lam, D.C.C., Tong, P. (2002). Couple stress based strain gradient theory for elasticity, Int J Solids Struct 39: 2731-2743.

Zhou, S.J., Li, Z.Q. (2001). Length scales in the static and dynamic torsion of a circular cylindrical micro-bar, J Shandong Univ Technol 31: 401-407.